



Published in final edited form as:

*Am J Obstet Gynecol.* 2016 September ; 215(3): 326.e1–326.e9. doi:10.1016/j.ajog.2016.03.023.

## Textile properties of synthetic prolapse mesh in response to uniaxial loading

Dr. William R. Barone, PhD, Dr. Pamela A. Moalli, MD, PhD, and Dr. Steven D. Abramowitch, PhD

Musculoskeletal Research Center, Department of Bioengineering (Drs Barone and Abramowitch), and Magee-Womens Research Institute, Magee-Womens Hospital (Drs Moalli and Abramowitch), University of Pittsburgh, Pittsburgh, PA

### Abstract

**BACKGROUND**—Although synthetic mesh is associated with superior anatomic outcomes for the repair of pelvic organ prolapse, the benefits of mesh have been questioned because of the relatively high complication rates. To date, the mechanisms that result in such complications are poorly understood, yet the textile characteristics of mesh products are believed to play an important role. Interestingly, the pore diameter of synthetic mesh has been shown to impact the host response after hernia repair greatly, and such findings have served as design criteria for prolapse meshes, with larger pores viewed as more favorable. Although pore size and porosity are well-characterized before implantation, the changes in these textile properties after implantation are unclear; the application of mechanical forces has the potential to greatly alter pore geometries in vivo. Understanding the impact of mechanical loading on the textile properties of mesh is essential for the development of more effective devices for prolapse repair.

**OBJECTIVE**—The objective of this study was to determine the effect of tensile loading and pore orientation on mesh porosity and pore dimensions.

**STUDY DESIGN**—In this study, the porosity and pore diameter of 4 currently available prolapse meshes were examined in response to uniaxial tensile loads of 0.1, 5, and 10 N while mimicking clinical loading conditions. The textile properties were compared with those observed for the unloaded mesh. Meshes included Gynemesh PS (Ethicon, Somerville, NJ), UltraPro (Artisyn; Ethicon), Restorelle (Coloplast, Minneapolis, MN), and Alyte Y-mesh (Bard, Covington, GA). In addition to the various pore geometries, 3 orientations of Restorelle (0-, 5-, 45-degree offset) and 2 orientations of UltraPro (0-, 90-degree offset) were examined.

**RESULTS**—In response to uniaxial loading, both porosity and pore diameter dramatically decreased for most mesh products. The application of 5 N led to reductions in porosity for nearly all groups, with values decreasing by as much as 87% ( $P < .05$ ). On loading to 10 N of force, nearly all mesh products that were tested were found to have porosities that approached 0% and 0 pores with diameters  $>1$  mm.

---

Corresponding author: Steven D. Abramowitch, PhD. [sdast9@pitt.edu](mailto:sdast9@pitt.edu).

W.R.B. reports no conflict of interest; P.A.M. and S.D.A. have a Cooperative Research Agreement ACELL.

Presented at the American Urogynecological Society Annual Meeting, Las Vegas, NV, October 16–19, 2013.

**CONCLUSION**—In this study, it was shown that the pore size of current prolapse meshes dramatically decreases in response to mechanical loading. These findings suggest that prolapse meshes, which are more likely to experience tensile forces in vivo relative to hernia repair meshes, have pores that are unfavorable for tissue integration after surgical tensioning and/or loading in urogynecologic surgeries. Such decreases in pore geometry support the hypothesis that regional increases in the concentration of mesh leads to an enhanced local foreign body response. Although pore deformation in transvaginal meshes requires further characterization, the findings presented here provide a mechanical understanding that can be used to recognize potential areas of concern for complex mesh geometries. Understanding mesh mechanics in response to surgical and in vivo loading conditions may provide improved design criteria for mesh and a refinement of surgical techniques, ultimately leading to better patient outcomes.

### Keywords

prolapse; pore diameter; porosity; synthetic mesh

---

Synthetic mesh use in the surgical repair of pelvic organ prolapse is widespread, with approximately one-third of all surgical repairs using mesh.<sup>1</sup> Ideally, synthetic mesh provides structural support to the vagina to eliminate the symptoms of prolapse, restore vaginal function, and relieve the psychosocial issues that result from this disorder.<sup>2,3</sup> Although synthetic mesh– augmented prolapse repairs boast superior anatomic outcomes relative to repairs that use native tissues, the benefit of mesh has been questioned because of complication rates that are as high as 20%, with notable rates of pain and mesh exposure (Figure 1, a).<sup>4-5</sup>

In an attempt to define the mechanism of complications,<sup>6,7</sup> significant focus has been placed on the textile properties of mesh. Specifically, the geometry and dimensions of the mesh pores have been found to impact the biologic response to mesh directly.<sup>8-11</sup> Indeed, greater pore sizes were found to yield mesh-tissue composites of greater strength and increased collagen deposition; smaller pores restricted vascular growth and contained less mature collagen.<sup>10,11</sup> Notably, it has been shown that effective tissue in-growth, which is characterized by the quality of the tissue that forms between mesh fibers, occurs in mesh pores with a diameter of  $\geq 1$  mm for polypropylene mesh.<sup>12</sup> Importantly, pore diameters of  $<1$  mm are associated with an enhanced inflammatory response that accompany poor tissue in-growth and fibrotic encapsulation.<sup>13,14</sup> Thus, it is not surprising that nearly all contemporary vaginal mesh products are constructed with initial pore diameters of  $>1$  mm. Yet, despite this design feature, it is not uncommon for mesh to appear bunched after implantation, particularly in areas of complications (Figure 1, b).

The apparent deformation of prolapse meshes highlights the need to consider the mechanical environment in which mesh is placed. Specifically, both abdominal sacrocolpopexy and trans-vaginal procedures anchor mesh (or mesh arms) at 2 distinct locations (vagina and sacrum or vagina and pelvic sidewall, respectively). Thus, when surgically tensioned to remove the presence of a vaginal bulge or loaded by other pelvic organs and/or abdominal pressure, the mesh largely experiences unidirectional (uniaxial) tensile loads along significant regions of the device (Figure 2). In response to this loading condition, one would

anticipate pore geometries to deform readily as the load is increased. Such loading previously has been shown to reduce mesh porosity.<sup>15</sup> Therefore, surgical tensioning and/or in vivo mechanical loading may provide a potential mechanism to explain clinical observations, often described as “mesh shrinkage.”<sup>16,17</sup>

Although previous studies have performed mechanical testing of synthetic mesh, many of these report data that are related to mesh failure (ie, begins tearing apart).<sup>18,19</sup> However, mechanical failure of synthetic mesh products is extremely rare clinically, because the typical failure properties of mesh far exceed in vivo loads and deformations. Rather, this study aims to characterize pore deformation at levels of force that occur in vivo and during surgical implantation, while considering the impact of initial pore orientation. We hypothesize that, regardless of initial pore geometry, mesh pores will become unsuitable for effective tissue ingrowth (dimensions, <1 mm) with decreased porosity on tensile loading.

## Materials and Methods

Four synthetic mesh products with distinct pore geometries were considered: Gynemesh PS (Ethicon, Somerville, NJ), UltraPro (aka Artisyn; Ethicon), Restorelle (Coloplast, Minneapolis, MN), and Alyte Y-mesh (Bard, Covington, GA; Table 1). Each product was cut to 90×15 mm strips along their recommended implantation direction. Multiple orientations were considered for several mesh products based on pore geometry and anticipated loading conditions for current sacrocolpopexy and transvaginal meshes. Specifically, Ultra-Pro was loaded with mesh cut at 0- and 90-degree offset from the recommended direction (labeled herein as UltraPro and UltraPro<sub>Opp</sub>, respectively). Because the initial pore geometry of Restorelle is square, porosity was not expected to change significantly in response to loading along this implantation direction. However, loading the mesh along an axis 45-degree offset to the square configuration (ie, tensioning a diamond shape pore) was expected to result in significant deformation. Therefore, Restorelle samples were cut in 3 orientations: pores offset at 0-, 5-, and 45-degrees from the horizontal axis. The 0- and 45-degree orientations were chosen based on geometry but were further justified by the anticipated loading of current transvaginal product designs (DirectFix; Figure 2), for which loading along these angles does occur. The 5-degree offset is clinically relevant, because small changes in orientation are likely to occur during implantation or cutting of the mesh.

Additionally, the intact Alyte mesh consists of 2 distinct sections; a section for vaginal attachment and a section intended for sacral attachment (Table 1). Although the general architecture is similar between the 2 locations, the sacral section consists of 2 offset layers of the vaginal section, which are knitted together. This construction effectively doubles the amount of material in the sacral section. Thus, samples from the vaginal and sacral sections were considered independently and demonstrate the impact of increased material on the deformation of mesh pores. Five samples that represented each of these aforementioned groups were independently tested.

The uniaxial testing apparatus and methods used have been described previously<sup>20,21</sup> All samples were secured in custom soft-tissue clamps on a materials testing machine (Instron

5565, Grove City, PA) such that the minimum clamp-to-clamp distance was 75 mm, which provided a minimum aspect ratio of 5. To remove slack, samples were preloaded to 0.1N at a rate of 10 mm/min. After the preload was applied, each mesh was loaded to 5N at 50 mm/min and subsequently to 10N at 50 mm/min. Neither force nor elongation measurements were zeroed between loading steps. Based on reported intraabdominal pressure and our measurements of surface area for the anterior vagina, the loads used in this protocol were within the estimated range of in vivo loads (eg, valsalva, coughing) placed on vaginal tissue.<sup>22,23</sup> We estimated <5N of force at resting intraabdominal pressure, although load values vary with vaginal dimensions, patient-specific abdominal pressures, or level of activity (ie, resting, jumping, coughing).

After the application of each load (preload included) the mesh mid region was imaged with the use of a digital SLR camera (EOS Rebel T3; Canon, Melville, NY) that was equipped with a 60-mm macro lens (EFS f/2.8; Canon). To produce repeatable image quality, all images were taken with high aperture (F16) and low ISO settings (ISO 100). In addition, all samples were imaged before testing, which provided 4 loading states for each mesh (0, 0.1, 5, and 10N). From each image, pore geometries were analyzed with a 10×10 mm section of the mesh midregion. The dimensions used for image analysis captured the repeating unit structure (pore geometry) of each mesh used in this study, but they were small enough to minimize the influence of the fixed boundaries imposed by the testing clamps, because larger porosity values would be observed closer to the clamps. Images were scaled and cropped using ImageJ (National Institutes of Health, Bethesda, MD) and then imported into a custom Mathematica script (V9, Champaign, IL). Images were then binarized with a thresholding procedure to ensure that all mesh fibers were included in analysis (Figure 3).

After thresholding, mesh porosity and the pore diameters were determined. To measure porosity, each image pixel was determined to be either mesh (Figure 3, black pixels) or void space (Figure 3, white pixels), which allowed for porosity to be calculated as:

$$\text{Porosity} = \text{void pixels} / \text{total pixels}$$

Porosity is a relative measure of the amount of mesh material per unit area, with a value of 0 representing a solid piece of mesh (no pores) and a value of 1 representing no mesh. To determine pore diameter, an algorithm was used to identify isolated clusters of white pixels (pores) and to calculate the centroid for each cluster. For each pore, the shortest distance, or minimum diameter ( $d_{\min}$ ), was recorded, creating a continuous distribution of  $d_{\min}$  for all pores in an image.

To display trends in pore diameter more easily, histograms were created such that  $d_{\min}$  values were grouped into 4 classes from 0–2 mm with a bin range of 0.5 mm. The contribution of each  $d_{\min}$  class to the total pore area was reported as the area fraction, where *area fraction* was defined as the pixel area of pores from a given diameter class divided by the total pore area in an image. Because of the lateral contraction of the mesh samples in response to tensile loading, void space outside of the mesh boundaries was not included for porosity measurements. Further, to avoid skewing of  $d_{\min}$  measurements, pores that were identified along the image perimeter were excluded from analysis.

Structural properties were computed for each mesh based on the load-elongation data that were obtained during testing. Here, elongation refers to the mesh elongation that resulted from the applied load. Stiffness measurements were made considering the nonlinearity of these curves as previously described.<sup>24</sup> The stiffness measurement, defined as the *low stiffness*, was calculated by taking the minimum slope of the load-elongation curve with a moving window of 5% elongation; *high stiffness* was calculated as the maximum slope of the curve with a 5% window. During imaging at 5N, each mesh experienced stress relaxation with the observed load decreasing to approximately 3N. This stress relaxation, which likely results from small changes in the knot structure, produced large initial stiffness values for 10N trials. Given the elevated initial stiffness for 10N trials, only structural properties from 0–5N were reported.

For statistical analysis, a repeated measures analysis of variance with Bonferroni post-hoc was used to examine the effect of loading on mesh porosity. The impact of loading on  $d_{\min}$  was examined using a Kruskal-Wallis test. Finally, the structural properties were compared between groups with a 1-way analysis of variance with Bonferroni or Dunnett's T3 post-hoc, as appropriate. Statistics were performed with SPSS software (V20; IBM Corporation, Armonk, NY), with a significance set at a probability value of .05.

## Results

Before being mounted in our testing system (0N), all meshes had pore sizes significantly  $>1$  mm and porosities  $>50\%$  (Table 1); however, uniaxial loading dramatically altered the overall appearance of mesh with notable changes in pore geometry (Figure 4). At 0N Gynemesh and Alyte's sacral portion had the lowest porosities (60.1% and 49.7% respectively; Figure 5). Mounting these samples and applying a 0.1N preload resulted in small decreases in porosity for several groups that were not significant (Figure 5). On the other hand, the application of 5N led to highly significant changes in pore shape and porosity for nearly all groups, with values decreasing by as much as 87% of their original porosity. Restorelle 0-degree offset (square pore) was the only mesh whose porosity was not significantly reduced on application of load ( $P > .05$ ; Figure 5). At 5N, Restorelle 45-degree offset, UltraPro<sub>Opp</sub>, and Alyte vaginal section saw the largest reductions in porosity, decreasing to just 9.5%, 11.7%, and 14.5% porosity, respectively. Gynemesh and Restorelle 5-degree offset experienced less reduction, approximately an 8% decrease in porosity ( $P < .05$ ). At 10N of force, all mesh groups other than Restorelle 0-degree and Restorelle 5-degree offset experienced such large pore reductions that the mesh structure grossly appeared as a solid piece of polypropylene (Figure 4). The porosity values were now only 15.5%, 10.2%, 6.4%, 3.8%, and 8.6%, for Gynemesh, UltraPro<sub>Opp</sub>, Restorelle 45-degree offset, Alyte vaginal, and Alyte sacral, respectively (Figure 5).

Measurements of pore dimensions further demonstrated the alteration of pore geometry in response to uniaxial loading, because all meshes experienced a significant decrease in  $d_{\min}$  at 10N of force ( $P < .001$ ; Figure 6). At 0N, all Restorelle cuts were found to have approximately 94% of the total pore area derived from pores of  $d_{\min} >1$  mm. Conversely, at 0N, Alyte's stem had just 35.6% of the total pore area from pores  $>1$  mm. Because the stem section is less likely to contact vaginal tissue, it is noted that Alyte's vaginal section had the

next lowest area fraction from pores  $>1$  mm at 55%. Although the application of a preload did not significantly alter  $d_{\min}$  for meshes considered here, the application of 5N significantly shifted the  $d_{\min}$  distribution for all meshes other than Gynemesh, with the mode decreasing in all cases. The most striking result at 5N was the finding that Restorelle 45-degree offset, UltraPro in both orientations, and both Alyte sections had no pores with a  $d_{\min} >1$  mm. In fact, Restorelle 45-degree offset, UltraPro<sub>Opp</sub>, Alyte stem, and Alyte vaginal had  $>90\%$  of the total pore area remaining from pores with diameters  $<0.5$  mm. At 10N of force, pore diameters continued to decrease for all meshes, with Gynemesh having the most dramatic shift in  $d_{\min}$  distribution, reflecting the absence of pores with a  $d_{\min} >1$  mm.

Overall the trends and observations from the load-elongation data were consistent with our previous testing.<sup>20,24</sup> When we compared the elongation required for each mesh to reach 5N of force, Restorelle 45-degree offset required almost 27 mm of elongation, nearly twice that of most groups tested ( $P < .05$ ; Figure 7). Most striking was UltraPro<sub>Opp</sub>, which required 59 mm of elongation to reach 5N, nearly 55% more than Restorelle 45-degree ( $P < .0001$ ; Table 2). It is notable that both of these meshes reached approximately 40mm and 15mm of elongation, respectively, at just 1N of force. This compliant behavior is reflected in the low stiffness measures for these meshes, which were an order of magnitude lower than of nearly all other meshes ( $P < .0001$ ; Figure 7). When we combined these values with reported pore diameters and experimental observations, it is apparent Restorelle 45-degree offset and UltraPro<sub>Opp</sub> offer little resistance to elongation, until the mesh pores have almost completely collapsed.

Conversely, Gynemesh was found to have the greatest low stiffness value at 0.30 N/mm, 2 times that of Restorelle 0-degree and nearly 4 times that of UltraPro ( $P < .0001$ ). The orientation of Restorelle dramatically altered its measured low stiffness. Similarly, an increased amount of material was found to increase the low stiffness measurement, because the initial stiffness of Alyte's stem was twice that of the vaginal section ( $P = .014$ ), which is consistent with the presumed manufacturer's intent to make the stem portion more resistant to deformation.

High stiffness values were more similar across all mesh groups, although significant differences were still observed. Alyte stem was found to have the greatest high stiffness value at 0.55 N/mm, which was 18% greater than Gynemesh ( $P = .001$ ) and 7% greater than the vaginal section of Alyte ( $P > .05$ ). Interestingly, Restorelle 5-degree had a decreased high stiffness value compared with 0-degree and 45-degree orientations, which were nearly identical. In addition, the high stiffness of UltraPro<sub>Opp</sub> was approximately 45% lower compared with UltraPro at 5N of force ( $P < .001$ ).

## Comment

In this study, changes in porosity and pore diameter of 4 currently available mesh products were examined in response to uniaxial tensile loading. It was observed that the changes in porosity and pore diameter, as well as the initial stiffness of a mesh, are dictated primarily by the pore geometry and the direction of applied force relative to this geometry. From a mechanical perspective, these general findings were expected and could have been predicted

without experimentation. However, a major finding of this study that was not anticipated was that the porosity of nearly all tested products approached 0% in response to just 10N of applied force, which is within the expected physiologic range and consistent with the forces we would expect meshes to experience before tissue incorporation (during implantation and in vivo). Additionally, this study found that the pore diameters of synthetic mesh are extremely sensitive to uniaxial forces; by 10N nearly all meshes that were tested had 0 pores with a diameter >1 mm. The determination of  $d_{\min}$  provides a clinically relevant parameter because diameters <1 mm are associated directly with a negative host response for polypropylene meshes.<sup>10,11</sup>

When these results are being considered with respect to clinical outcomes, it should be noted that the ex vivo behavior observed in this study is analogous to mesh behavior at the time of implantation and before tissue integration. These findings are critical to consider when initially placing/tensioning a mesh and when the mechanical demands required for a specific patient (ie, obese patients, orientation of vaginal axis, patients who perform regular heavy lifting). Given the importance of pore diameters, deformation at the time of and early after implantation likely dictates the subsequent response and integration of synthetic mesh. It can be hypothesized that decreases in pore diameter enhance the host inflammatory response and possibly increase the fibrous encapsulation of the mesh. Fibrous encapsulation and its potential contraction by resident myofibroblasts may induce pain after mesh implantation, which is 1 of the most common of mesh-related complications.<sup>25</sup>

Further, this study found that reporting mesh pore size as a single diameter is misleading. On measurement, mesh products contain a range of pore diameters, with “large pore” meshes (diameters >1 mm) also have a large number of small pores that are more likely to evoke a fibrotic immune response. The present study only considers macropores because the smallest pore size that we were able to resolve with our methods was on the order of 0.02 mm. However, the host response to a particular mesh is also dictated by micropores (on the order of 0.001 mm), which are very likely to increase in number as pores collapse. In future studies, characterization of micropores should be performed alongside macroscopic analyses to understand thoroughly the entire host response to prolapse mesh.

Additionally, it should be noted that the loading conditions that were used in this study were simplified relative to the in vivo mechanical environment. Given our limited understanding of the complex mechanical environment of the pelvic floor, the simplified conditions used here allowed for comparison of meshes and differing pore geometries in a controlled manner. Clinically, a number of variables that included the degree and site of prolapse, surgical technique, suture placement, and patient size influence pore deformation. Still the work presented here is most representative of meshes that are used in sacrocolpopexy, because these are largely loaded in tension. Extrapolating these results to transvaginal devices is more difficult and requires advanced experimental and computational methods. Nonetheless, the behavior exhibited here provides a basic understanding of how mesh deforms in response to load and can be used to make an educated guess as to the behavior of transvaginal devices and to develop more advanced analyses.

Previous studies have found that high stiffness mesh results in increased deterioration of vaginal tissue after implantation, leading to increased clinical use of low stiffness prolapse meshes.<sup>26</sup> However, given the importance of pore size, the stiffness of a mesh must be balanced with its ability to maintain pore diameters >1 mm. Although it may seem intuitive that a stiff mesh, such as Gynemesh PS, is more likely to retain large pore diameters, this study shows that pore geometry and direction of the applied load with respect to the pore geometry are also critical factors. Although all current prolapse meshes will likely experience a complete collapse of pores at some load, maintenance of pore diameters within the range in vivo loads should be considered an important design feature for mesh devices in conjunction with stiffness.

Finally, it should be noted that the accuracy of the measurements in this study are subject to the quality of the images that were obtained during testing. Although a large depth of field was used to produce sharp images, out-of-plane fiber deformation may result in image blurring, which artificially increases the porosity (decreasing  $d_{\min}$ ) of the mesh. Additionally, binarization and thresholding protocols may be subject to image quality, because they require high contrast between the background and mesh fibers. To achieve repeatable results, the same background, lighting conditions, and camera settings were used for all images.

Future studies will be performed to analyze pore deformation of complex mesh geometries, such as those found in transvaginal mesh kits, in response to clinically relevant boundary conditions. In addition, pore deformation results will be used to create and validate computational models for mesh products. Such models will provide invaluable tools in the development and optimization of future mesh products.

## Acknowledgments

Supported by a grant from the National Institutes of Health, R01HD061811, by the National Science Foundations Graduate Research Fellowship award DGE-0753293 and National Institutes of Health, grants R01 HD-061811 and K12HD-043441 is appreciated.

## References

1. U.S. Food and Drug Administration. [Accessed April 25, 2016] Surgical placement of mesh to repair pelvic organ prolapse poses risks. Available at: <http://www.fda.gov/NewsEvents/Newsroom/PressAnnouncements/ucm262752.htm>
2. Maher C, Baessler K, Glazener C, Adams E, Hagen S. Surgical management of pelvic organ prolapse in women. *Cochrane Database Syst Rev.* 2007; 3:CD004014.
3. Ghetti C, Lowder JL, Ellison R, Krohn MA, Moalli P. Depressive symptoms in women seeking surgery for pelvic organ prolapse. *Int Urogynecol J Pelvic Floor Dysfunc.* 2010; 21:855–60.
4. Patel BN, Lucioni A, Kobashi KC. Anterior pelvic organ prolapse repair using synthetic mesh. *Curr Urol Rep.* 2012; 13:211–5. [PubMed: 22588645]
5. Bako A, Dhar R. Review of synthetic mesh-related complication in pelvic floor reconstructive surgery. *Int Urogynecol J Pelvic Floor Dysfunc.* 2008; 20:103–11.
6. Deffieux X, de Tayrac R, Huel C, et al. Vaginal mesh erosion after transvaginal repair of cystocele using Gynemesh or Gynemesh-Soft in 138 women: a comparative study. *Int Urogynecol J Pelvic Floor Dysfunc.* 2007; 18:73–9. [PubMed: 16391882]
7. Nygaard I, Barber MD, Burgio KL, et al. Prevalence of symptomatic pelvic floor disorders in US women. *JAMA.* 2008; 200:1311–6.



8. Chvapil M, Holuša R, Kliment K, Štoll M. Some chemical and biological characteristics of a new collagen–polymer compound material. *J Biomed Mater Res A*. 1969; 3:315–32.
9. Patel H, Ostergard D, Sternschuss G. Polypropylene mesh and the host response. *Int Urogynecol J Pelvic Floor Dysfunct*. 2012; 23:669–79.
10. Greca FH, De Paula JB, Biondo-Simões MLP, et al. The influence of differing pore sizes on the biocompatibility of two polypropylene meshes in the repair of abdominal defects: experimental study in dogs. *Hernia*. 2001; 5:59–64. [PubMed: 11505649]
11. Greca FH, Souza-Filho ZA, Giovanini A, et al. The influence of porosity on the integration histology of two polypropylene meshes for the treatment of abdominal wall defects in dogs. *Hernia*. 2008; 12:45–9. [PubMed: 17823771]
12. Klinge UKB. Modified classification of surgical meshes for hernia repair based on the analysis of 1000 explanted meshes. *Hernia*. 2011; 16:251–8.
13. Weyhe D, Schmitz I, Belyaev O, et al. Experimental comparison of monofilament light and heavy polypropylene meshes: less weight does not mean less biological response. *World J Surg*. 2006; 30:1586–91. [PubMed: 16855805]
14. Bellon LM, Jurado F, Garcia-Honduvilla N, Lopez R, Carrera-San Martin A, Bujan J. The structure of a biomaterial rather than its chemical composition modulates the repair process at the peritoneal level. *Am J Surg*. 2002; 184:154–9. [PubMed: 12169360]
15. Otto J, Kaldenhoff E, Kirschner-Harmanns R, Muhl T, Klinge U. Elongation of textile pelvic floor implants under load is related to complete loss of effective porosity, thereby favoring incorporation in scar plates. *J Biomed Mater Res A*. 2014; 102:1079–84. [PubMed: 23625516]
16. Svabík K, Martan A, Masata J, El-Haddad R, Hubka P, Pavlikova M. Ultrasound appearances after mesh implantation - Evidence of mesh contraction or folding? *Int Urogynecol J Pelvic Floor Dysfunct*. 2011; 22:529–33.
17. Rogowski A, Bienkowski P, Tosiak A, Jerzak M, Mierzejewski P, Baranowski W. Mesh retraction correlates with vaginal pain and overactive bladder symptoms after anterior vaginal mesh repair. *Int Urogynecol J*. 2013; 24:2087–92. [PubMed: 23749240]
18. Dietz HP, Vancaillie P, Svehla M, Walsh W, Steensma AB, Vancaillie TG. Mechanical properties of urogynecologic implant materials. *Int Urogynecol J Pelvic Floor Dysfunct*. 2003; 14:239–43. [PubMed: 14530834]
19. Krause H, Bennett M, Forwood M, Goh J. Biomechanical properties of raw meshes used in pelvic floor reconstruction. *Int Urogynecol J Pelvic Floor Dysfunct*. 2008; 19:1677–81. [PubMed: 18762850]
20. Shepherd JP, Feola AJ, Abramowitch SD, Moalli PA. Uniaxial biomechanical properties of seven different vaginally implanted meshes for pelvic organ prolapse. *Int Urogynecol J Pelvic Floor Dysfunct*. 2012; 23:613–20.
21. Moalli PA, Papas N, Menefee S, Albo M, Meyn L, Abramowitch SD. Tensile properties of five commonly used mid-urethral slings relative to the TVT. *Int Urogynecol J Pelvic Floor Dysfunct*. 2008; 19:655–63. [PubMed: 18183344]
22. Cobb WS, Burns JM, Kercher KW, Matthews BD, Norton HJ, Heniford BT. Normal intraabdominal pressure in healthy adults. *J Surg Res*. 2005; 129:231–5. [PubMed: 16140336]
23. Noakes NF, Pullan AJ, Bissett IP, Cheng LK. Subject specific finite elasticity simulations of the pelvic floor. *J Biomech*. 2008; 41:3060–5. [PubMed: 18757058]
24. Jones KA, Feola A, Meyn L, Abramowitch SD, Moalli PA. Tensile properties of commonly used prolapse meshes. *Int Urogynecol J Pelvic Floor Dysfunct*. 2009; 20:847–53. [PubMed: 19495548]
25. Crosby EC, Abemethy M, Berger MB, DeLancey JO, Fenner DE, Morgan DM. Symptom resolution after operative management of complications from transvaginal mesh. *Obstet Gynecol*. 2014; 123:134–9. [PubMed: 24463673]
26. Liang R, Abramowitch S, Knight K, et al. Vaginal degeneration following implantation of synthetic mesh with increased stiffness. *BJOG*. 2013; 120:233–43. [PubMed: 23240802]

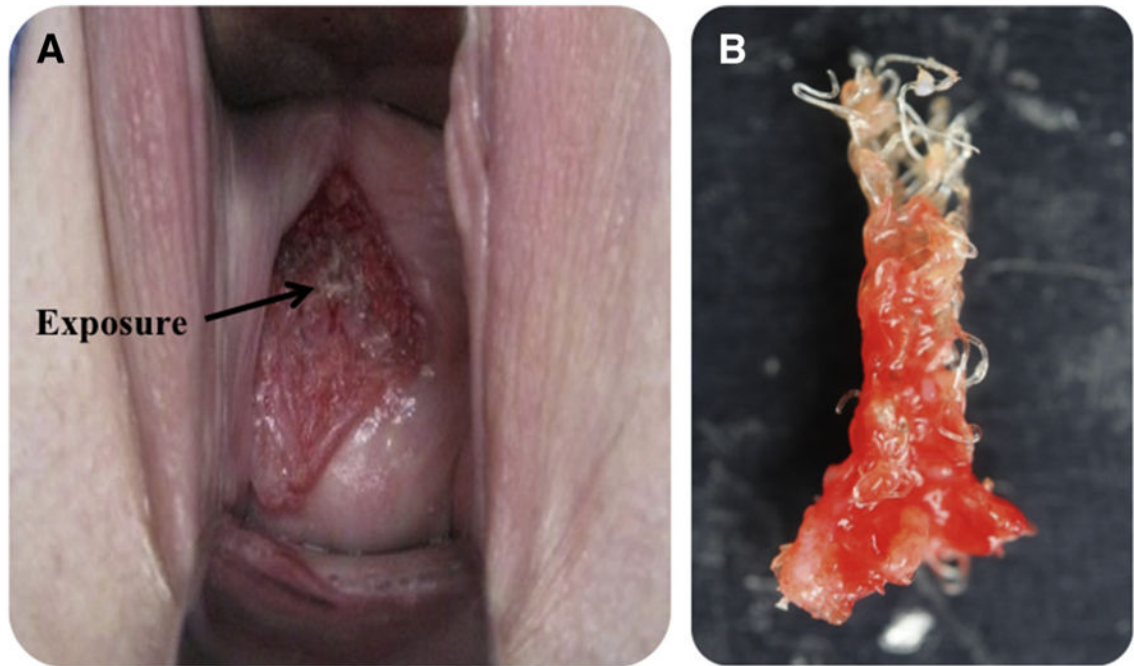


**FIGURE 1. Example of mesh exposure**

**A**, Mesh exposure characterized by visualization and palpation of mesh in the vaginal lumen. **B**, To treat exposure, mesh is often surgically removed. On removal, it is not uncommon for mesh to appear bunched, with noticeably altered pore geometries.

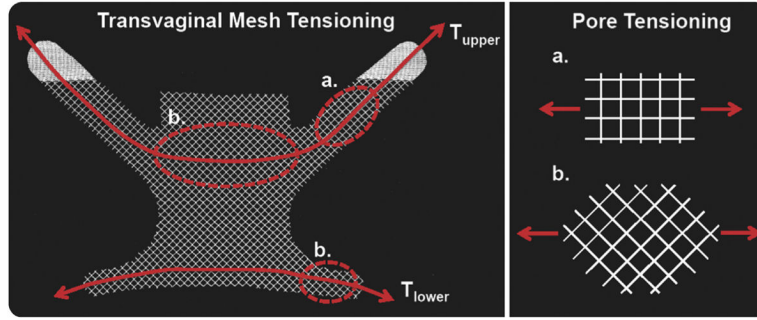


**FIGURE 2. Transvaginal prolapse mesh**

Transvaginal prolapse mesh is tensioned to remove the presence of a vaginal bulge. Tension applied to the upper ( $T_{upper}$ ) and lower ( $T_{lower}$ ) arms of a transvaginal mesh results in transmission of force throughout the entire device. Along the path of force transmission, the pore structure is loaded in various orientations. Shown here, Restorelle's square pores are loaded at approximately 0-degree offset in the upper mesh arms; pores at the center of the mesh and in the lower arms are likely tensioned at approximately 45-degrees offset.

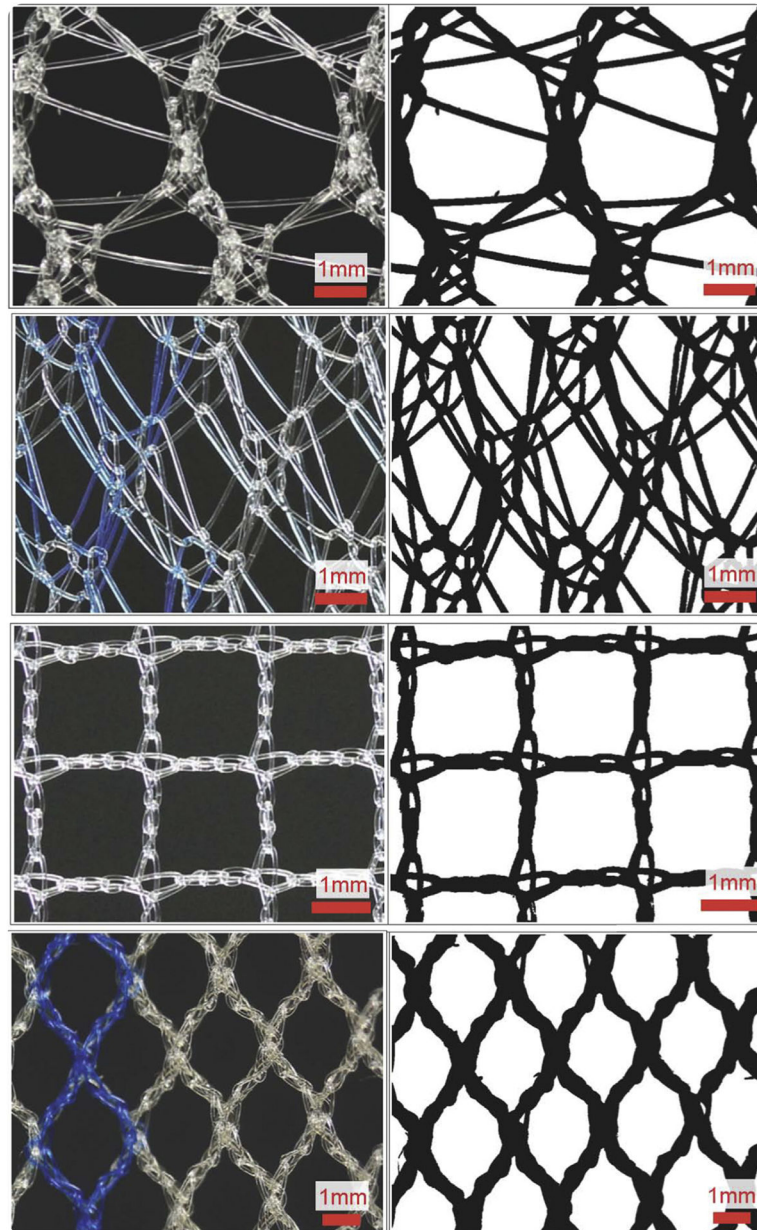


**FIGURE 3. Raw images and corresponding binarized images**

Raw images (*left*) and corresponding binarized images after custom thresholding protocol (*right*). In order from top to the bottom are unloaded (0N) mesh mid region images of Gynemesh, Alyte's stem section, Restorelle 0-degree offset, and UltraPro (Artisyn).

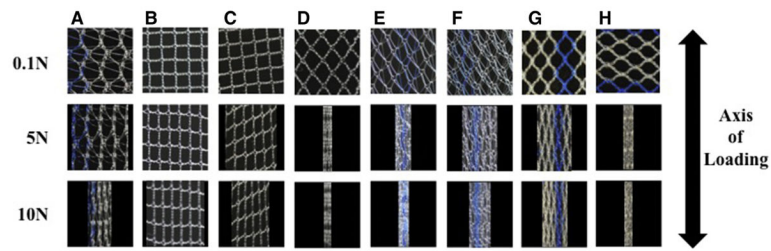


**FIGURE 4. Raw images of mesh mid region deformation**

Raw images of mesh mid region deformation at 0.1N (*top*), 5N (*middle*), and 10N (*bottom*) of applied force. Representative images from **a**, Gynemesh, **b**, Restorelle 0-degree, **c**, Restorelle 5-degree, **d**, Restorelle 45-degree, **e**, Alyte's vaginal section, **f**, Alyte's stem section, **g**, UltraPro, and **h**, UltraPro<sub>Opp</sub> are shown. Each image has dimensions of 10 × 10 mm.

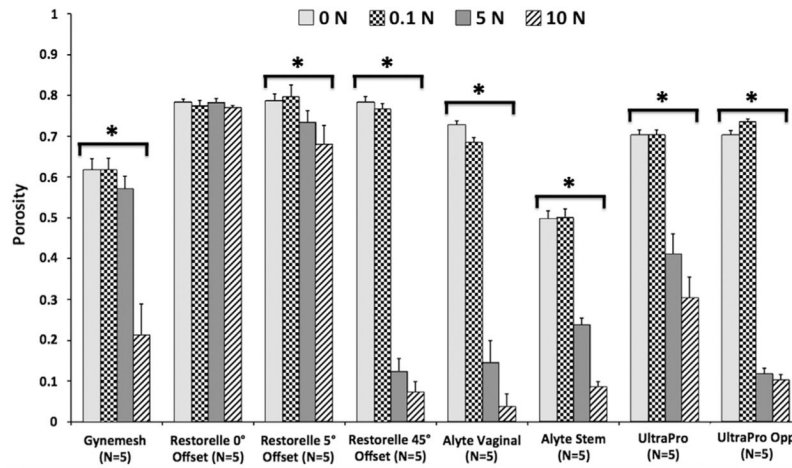


**FIGURE 5. Impact of uniaxial loading on mesh porosity**  
 Porosity measurements for each mesh group at 0, 0.1, 5, and 10N of uniaxial tension. *Error bars* represent standard deviation; the *asterisks* represent a significant impact of loading on mesh porosity ( $P < .05$ ).

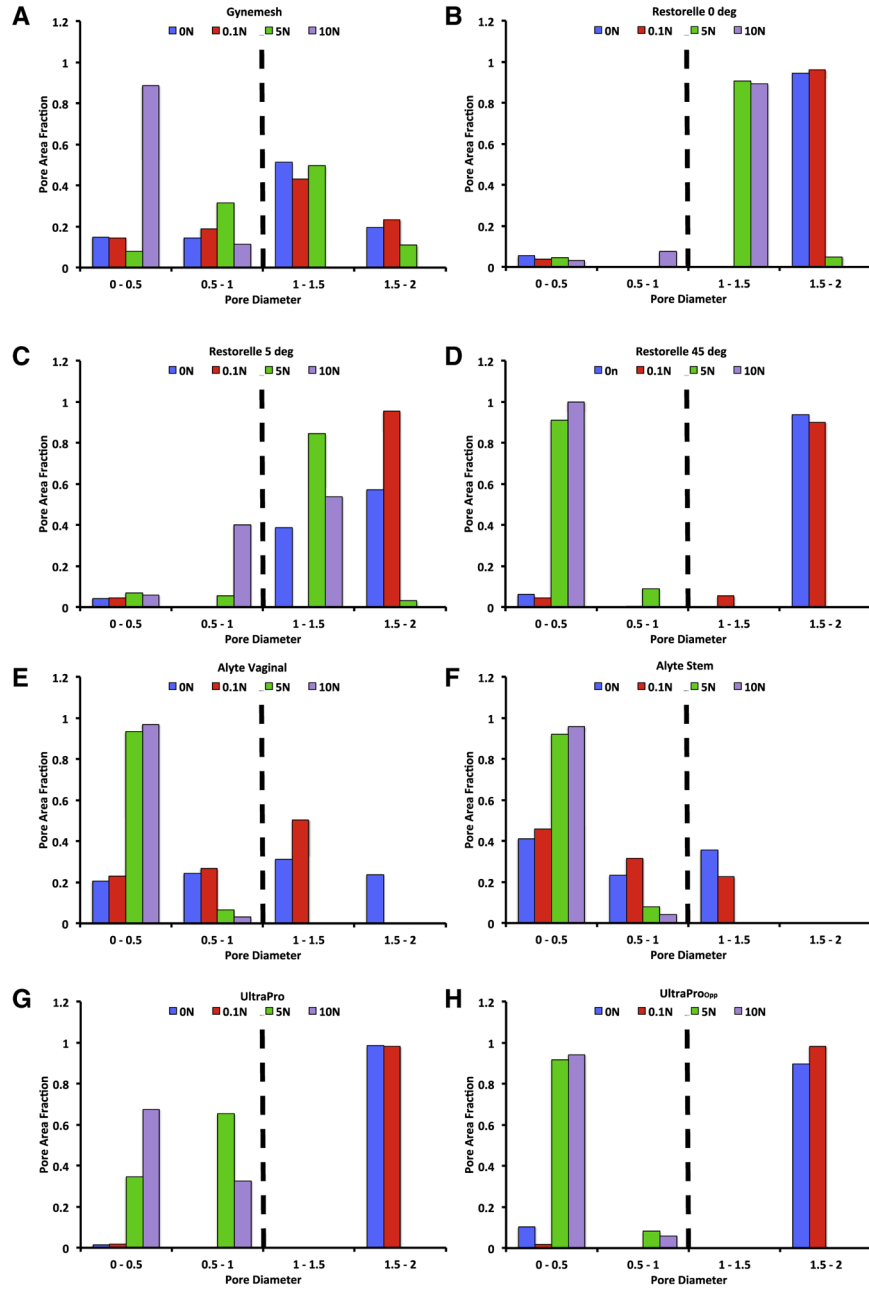


**FIGURE 6. Distribution of minimum pore diameter**  
 Distribution of minimum pore diameter ( $d_{min}$ ) for **a**, Gynemesh, **b**, Restorelle 0-degree, **c**, Restorelle 5-degree, **d**, Restorelle 45-degree, **e**, Alyte’s vaginal section, **f**, Alyte’s stem section, **g**, UltraPro, and **h**, UltraPro<sub>Opp</sub> at 0, 0.1, 5, and 10N of force. The *y-axis* represents the fraction of total pore area contributed by pores within a given range of diameters. The application of a uniaxial load was found to alter diameter distribution significantly for all meshes that were tested ( $P < .05$ ).

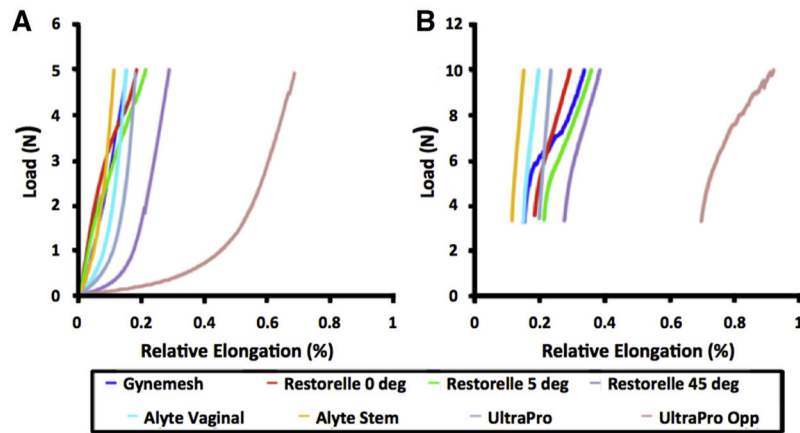


**FIGURE 7. Representative load-elongation curves for all groups tested**

Meshes display a wide range of responses from 0–5N, **a**, because of initial pore geometry and orientation of mesh fibers along the loading axis. **b**, Because of the time required to image samples at 5N, each mesh underwent stress relaxation before application of 10N of load.



**TABLE 1**

Industry-reported textile properties of tested mesh before loading

Mesh	Vendor	Pore size, mm	Porosity, %
Gynemesh	Ethicon	2.5	62
Restorelle	Coloplast	1.8	78
Alyte Vaginal	Bard	2.8	75
Alyte Stem	Bard	2.0	50
UltraPro <sup>a</sup>	Ethicon	3.8	68

For competitive comparisons, manufacturers typically report pore size and porosity with the mesh in an unloaded state. In addition, it should be noted that manufacturers report a single value for pore size, typically the largest diameter in the mesh structure, although all prolapse meshes contain a wide range of pore sizes.

<sup>a</sup>UltraPro (aka Artisyn) measurements made after absorbable component is absorbed.

Author Manuscript

Author Manuscript

Author Manuscript

Author Manuscript

**TABLE 2**

Structural properties for each mesh obtained from load-elongation curves to 5N

Mesh (n = 5 each)	Elongation, mm±SD	Low stiffness, N/mm±SD	High stiffness, N/mm±SD
Gynemesh	12.78 ± 0.00	0.30 ± 0.01	0.45 ± 0.02
Restorelle 0-degree	16.00 ± 0.03	0.16 ± 0.07	0.41 ± 0.06
Restorelle 5-degree	17.42 ± 0.03	0.23 ± 0.03	0.32 ± 0.04
Restorelle 45-degree	26.70 ± 0.06	0.02 ± 0.01	0.42 ± 0.03
Alyte Vaginal	12.67 ± 0.01	0.12 ± 0.01	0.51 ± 0.02
Alyte Stem	9.76 ± 0.01	0.24 ± 0.04	0.55 ± 0.02
UltraPro	14.41 ± 0.01	0.08 ± 0.01	0.49 ± 0.02
UltraPro <sub>Opp</sub>	59.25 ± 0.02	0.01 ± 0.01	0.27 ± 0.02
Overall probability value	.001	.000	.029

Elongation values are those that resulted from 5N of force being applied to the mesh; low and high stiffness values are the minimum and maximum slopes of the load-elongation curve, respectively. To minimize the complexity of this Table, relevant probability values for individual comparisons are reported in the text.